Algorithms for Real-Time Acquisition and Segmentation of a Stream of Thermographic Line Scans in Industrial Environments

Rubén Usamentiaga†, Daniel F. García and Carlos López
University of Oviedo, Gijón, Asturias, SPAIN

Juan A. González
Aceralia Steel Corporation, Avilés, Asturias, SPAIN

This article presents a system for acquisition, filtering, and segmentation of thermographic images in real time. Image acquisition is carried out using an infrared line scanner (IRLS), with which thermographic line scans are captured from hot strips while they are moving forward along a track. During the acquisition process, a relationship between each sample in the line scan and its position on the strip is established using a theoretical model of the IRLS, whose parameters have been adjusted using a calibration procedure. After the acquisition, line scans are filtered using a new signal operator designed to work in real time. Online with acquisition and filtering processes, segmentation is applied to the stream of line scans to group them into regions with similar temperature pattern. Two new segmentation algorithms based on well-known approaches, region merging and edge detection, have been designed to work in real time on a stream of line scans. The algorithms are evaluated using a novel segmentation assessment method based on the uncertainty of the ground truth, which can also be used for parameter tuning. Experimental results from a database of 200,000 images taken from manufactured steel strips over a period of three years demonstrate the efficiency and effectiveness of the proposed system.

Journal of Imaging Science and Technology 49: 138–153 (2005)

Introduction

In recent decades, much research effort has been centered on the real time image processing field, where the processed images are taken mostly from the human visible spectrum. Real time thermographic image processing is a branch of the signal processing tree with some similarities to traditional image processing. However, due to the lack of appropriate hardware, thermographic imaging has been often neglected, except in some specific cases such as military applications.[1] Recently, fast and affordable hardware has been developed making the use of thermography possible in a new variety of real time applications. One of these applications is real time thermographic imaging applied to continuous hot material, such as steel strips manufactured on a production line.

Images taken of the human visible spectrum have been widely used in visual inspection applications.[2–4] However, the use of thermographic images in this field is not yet common. In this work several algorithms are proposed and evaluated for the real time acquisition, filtering and segmentation of thermographic images. All these algorithms work in real time, that is, on-line with the production process, so that the control parameters of the production process could be modified as soon as an incorrect temperature pattern appears.

In the Acquisition process, temperature values from the surface of the material are obtained. Two hardware elements are used: a high speed IRLS (Infra-Red Line scanner), and an industrial computer which converts the temperature from an analog signal to digital samples with the help of an A/D acquisition card. A new procedure to associate the samples of a line scan to physical positions (mm) on the continuous material has been developed using a theoretical approach based on a model of the IRLS. The parameters of the IRLS model are adjusted using an empirical calibration procedure carried out before the system starts up.

The filtering process reduces the noise of the image in order to obtain a successful analysis in further steps of the image processing. Two consecutive filtering processes are used: a filtering process within each line scan based on oversampling of each line scan, and a low pass filtering process between successive line scans to smooth the final two-dimensional image.

The intra-scan filtering is carried out perpendicularly to the strip movement. This direction is called the

Original manuscript received July 6, 2004

†Corresponding Author: R. Usamentiaga, ruf@atc.uniovi.es

transversal direction in the final two-dimensional image. The inter-scan filtering is carried out in the same direction as the movement of the strip. This direction is called the longitudinal direction in the two-dimensional thermographic image.

The objective of real time segmentation is the detection of significant changes in the pattern of the thermographic line scans acquired. The set of line scans acquired between two pattern changes will be considered as a region of the final two-dimensional image. Two new segmentation algorithms based on well-known approaches, region merging and edge based, have been designed to work in real time on a stream of line scans. The algorithms are evaluated using a novel segmentation assessment method based on the uncertainty of the ground truth, which can also be used for parameter tuning.

Real time segmentation will detect changes in the line scan thermographic pattern of the strip. This information is very useful in the control loop of the manufacturing process since the information can be used to modify the manufacturing parameters in real time in order to reach a more stable temperature pattern. Stable temperature patterns produce high quality products, while non-uniform temperature patterns produce defects due to the different contractions of the material during the cooling. Changes in the temperature pattern will be detected through the real time segmentation allowing the feedback of a new pattern in the control loop of the manufacturing process.

Acquisition

The thermographic image is obtained using a high speed infrared line scanner (IRLS), which consists of a pyrometer which turns continuously at a frequency, F. The IRLS measures the energy radiated by the surface of an object. Using Plank radiation equations, the measured energy is converted to an analog signal which represents the temperature. This signal is sent to the computer through an electrical line in the range 4 – 20 mA. At every turn, the IRLS generates an analog signal which represents the temperature of a segment across the strip perpendicular to the direction of the strip movement.

The analog signal is sampled by a computer, resulting in a line scan (range 100– 200°C), that is, a set of samples in the range 100 – 200°C which correspond to the temperature measurements of a segment across the strip. The number of samples obtained in every line scan depends on the sampling acquisition rate used in the A/D converter installed in the industrial computer.

The analog signal representing the temperature contains valid data only while the rotating pyrometer inside the IRLS is pointing the track. In the IRLS used, that part of the turn, usually called the scan valid angle, represents 1/6 of the whole turn, that is, 60° (Fig. 1). A line scan is obtained through the sampling of the analog temperature signal only during the scan valid angle (Fig. 2). The IRLS notifies the computer the beginning and end of the scan valid angle through the activation (5 V) and deactivation (0 V) of a digital signal.

The repetitive sampling of the analog signal and the movement of the strip forward along a track, make the acquisition of temperature discrete samples over the whole surface of the strip possible. The image obtained consists of a stream of line scans corresponding to each analog signal sent by the IRLS while the strip moves forward along the track.

The image acquisition system must be calibrated before being started up. Procedures for the calibration

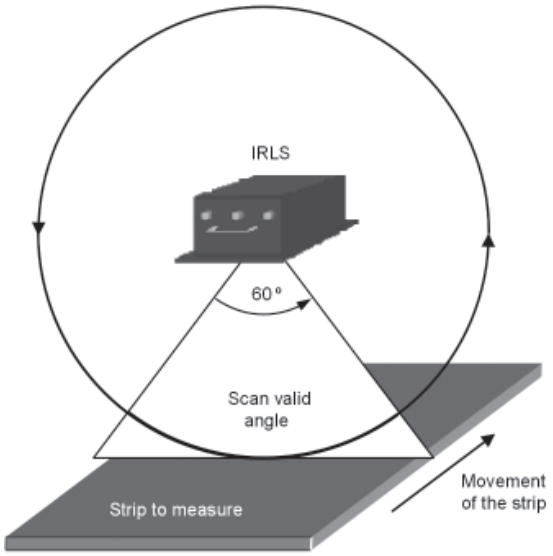

Figure 1. Temperature measurement over the strip surface.

of two scales, temperatures and positions, have been developed.

The temperature scale is calibrated using the emissivity parameter of the IRLS. The temperature provided by the IRLS is related to the temperature of the material through the black body radiation equation, in which the emissivity of the material is a proportionality factor. Emissivity settings in the range from 0.2 to 1.0 are supplied to the IRLS as one of its remote control input signals. When the emissivity parameter is decreased, the temperature provided by the sensor increases, and vice versa. An experiment was carried out in the laboratory in order to obtain the emissivity value for the material to be measured. The experiment parameter was based on the comparison of the temperature measured by the IRLS and the temperature measured by a previously calibrated contact thermometer, both of them obtained from the same piece of heated steel at the same time. The emissivity was modified in the IRLS until the temperature it provided matched the temperate provided by the contact thermometer. The result showed that suitable emissivity for this kind of measured material (thin steel) was 0.37. The experiment carried out was possible because the temperature range is low [100–200°C]. Obviously, this experiment would not be possible if the temperature range were higher, for example 1250°C, since there is no contact thermometer designed to work at these temperatures. Another kind of emissivity calibration experiment could be used in that case.[1]

The position scale calibration allows the association of each temperature sample within the line scan with its physical position on the strip. To obtain this association, a theoretical approach was developed using the geometry defined in Fig. 3. In this geometry, a line scan with N samples in the range $[0, N - 1]$ is used, where the working distance (from the IRLS to the strip) is D, the turn frequency of the IRLS is F and the scan valid angle is α. The turn frequency and the scan valid angle are known parameters defined by the IRLS. The objective is to calculate the distance from a single sample, J, in the line scan to the origin, O (distance between A and O, both referenced in Fig. 3). Although in an optimal situation the origin O should match the central point of the line scan B, the IRLS cannot be

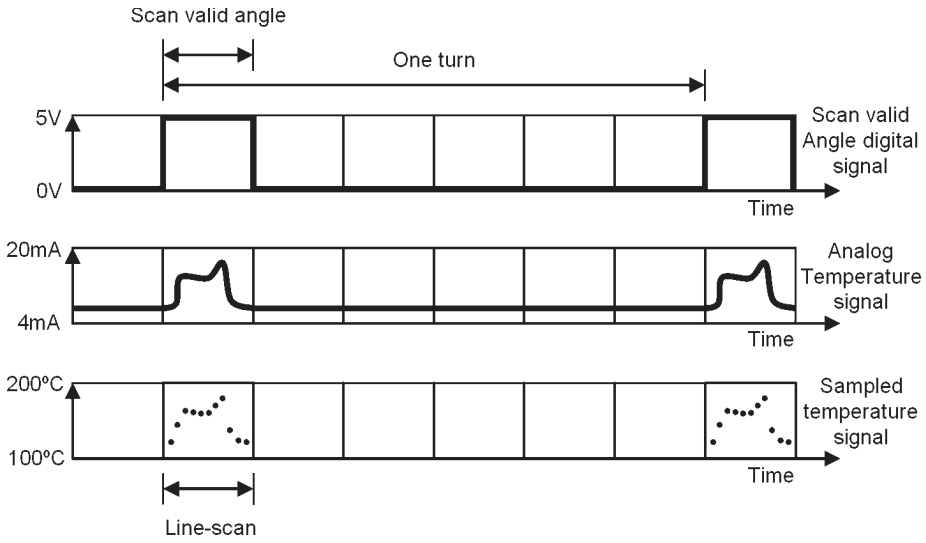

Figure 2. IRLS timing diagram.

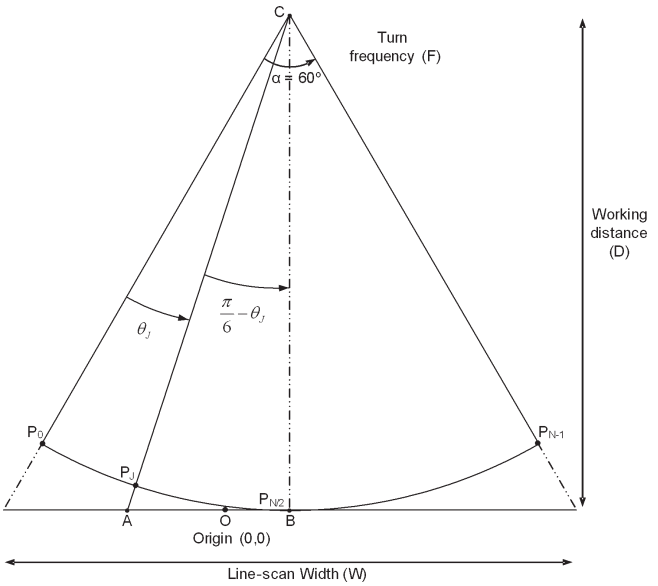

Figure 3. Geometry of the line scan acquisition process.

installed in the center of the track due to mechanical problems. For this reason, a non-centered origin is considered in the model.

The elapsed time during the scan valid angle, T, can be calculated using Eq. (1). The time interval from the start of the scan valid angle to the acquisition of sample J is a part of period T, and can be calculated using Eq. (2). The angle θ_J can be calculated using Eq. (3). By combining Eqs. (1) and (2) into Eq. (3), a simplified expression for θJ is reached in Eq. (4).

$$T = \frac{\left[\frac{1}{F}\right]}{\frac{360^\circ}{60^\circ}} = \frac{\left[\frac{1}{F}\right]}{6} = \frac{1}{6F} \tag{1}$$

$$t = \frac{J}{N}T \tag{2}$$

$$\theta_J = \frac{t}{T}60^\circ = \frac{t}{T}\frac{\pi}{3} \tag{3}$$

$$\theta_J = \frac{\frac{J}{N}T}{T}\frac{\pi}{3} = \frac{J}{N}\frac{\pi}{3} \tag{4}$$

Once the angular position, θ_J, of the sample J is known, the distance between A and B can be calculated using the properties of the right angle triangle whose sides are AB, BC and CA by Eq. (5).

$$d(A,B) = D * \tan(\frac{\pi}{6} - \theta_J) \tag{5}$$

In the same way, the distance between O and B can be calculated using Eq. (6), where θ_O is the angular position of origin O.

$$d(O,B) = D * \tan(\frac{\pi}{6} - \theta_O) \tag{6}$$

Finally, Eq. (7) gives the distance between A and O.

$$d(A,O) = d(A,B) - d(O,B) = D\left[\tan(\frac{\pi}{6} - \theta_J) - \tan(\frac{\pi}{6} - \theta_O)\right] \tag{7}$$

The distance from every sample in the line scan to the origin is obtained using Eq. (7). This final equation has two unknown parameters: the working distance (D) and the angular position of the origin (θ_O). These parameters will be estimated using an empirical calibration procedure, which is briefly described below.

In order to calculate the working distance (D), an empirical calibration procedure was carried out on the track of the production line where the IRLS is installed. During the calibration, a hot resistance with sharp edges was placed in known positions along the scanning trajectory (turn) of the IRLS. This process is shown in Fig. 4, where the heated resistance is drawn in only four different positions for the sake of simplicity. In the experiment 15 different positions were used starting at

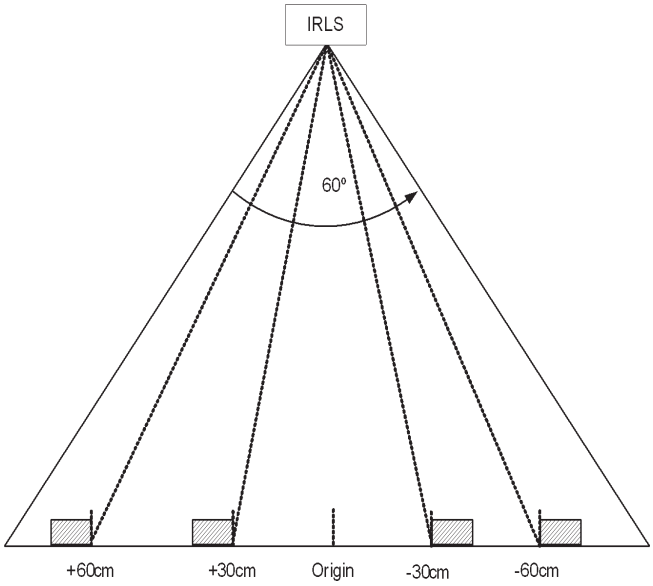

Figure 4. Empirical calibration through the placement of a hot resistance in the IRLS turn trajectory.

+70 cm from the origin and shifting the object every 10 cm until −60 cm (this asymmetry is due to the displacement of the IRLS to the left of center). Positive values are shown on the left to be consistent with other measurements carried out in the area in which the IRLS is installed.

Each time the hot resistance was placed in a known position, a line scan was obtained. The line scans produced at the different placements of the hot resistance in the trajectory of the IRLS are shown in Fig. 5.

For each line scan obtained after each placement of the hot resistance, the Ridler thresholding technique[5] is applied to calculate the position of the edge. Each thresholding applied to a line scan provides two edges, but only the one in the interior part (marked as I in Fig. 5) will be used in order to avoid the error provoked by the slanting viewpoint. Finally a lookup table is obtained relating samples and their physical position (mm across the track). The position at zero is measured twice (+0 and −0) to confirm position of the origin.

Using the lookup table obtained during the empirical calibration, the angular position of the origin can be obtained easily as the sample at the origin is now known. The second unknown parameter in the theoretical approach was the working distance, which can be calculated as the value which minimizes the difference between the position of the samples reported in the empirical calibration procedure and the position calculated for those samples using the theoretical approach. Using the proper working distance, the relationship between samples and physical positions can be obtained from Eq. (7), which is represented in Fig. 6(a). The curvature of the function can be observed in more detail in Fig. 6(b), where the distance between adjacent samples is represented. It can be seen, the further the sample is from the center of the line scan, the longer the distance to its adjacent samples.

After establishing the position of the samples across the strip (within a line scan), the next step is to obtain their position along the strip. To obtain the longitudinal position of the samples, the way in which a line scan is acquired must be kept in mind. The line scan acquisition is shown in Fig. 7, where it can be seen that the line scan is not perpendicular to the strip due to the movement of the strip.

In Eq. (8), i is the sample number in the line scan, V is the speed of the strip, F is the turn frequency of the IRLS, N is the number of samples in the line scan and L_0 is the longitudinal position of the line scan starting sample, which will be received, along with the speed of the movement of the strip, from the process computer during the acquisition. This equation is used to calculate the longitudinal position of every sample in the line scan.

$$L[i] = L_0 + \frac{V\dfrac{1}{6F}}{N} i \tag{8}$$

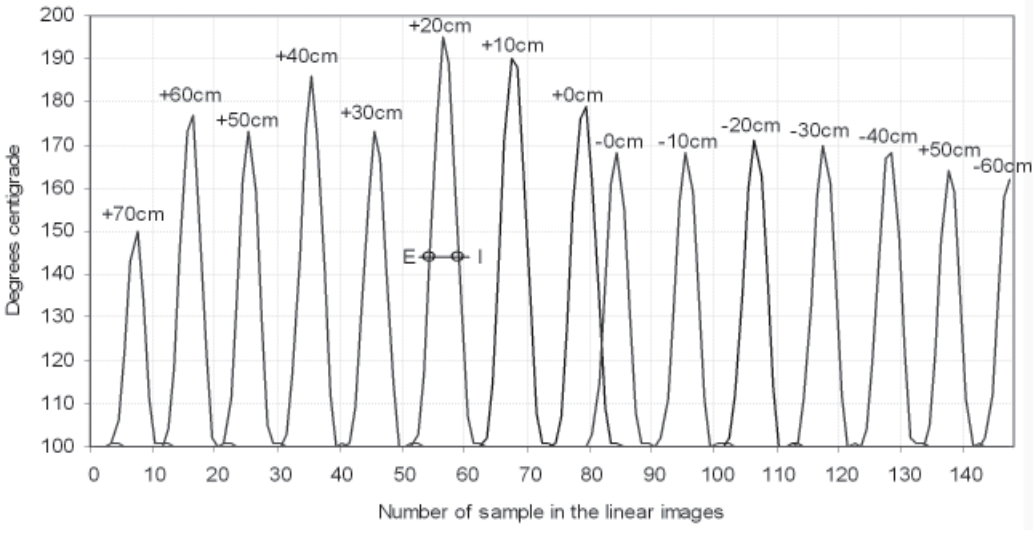

Figure 5. Line scans obtained during the empirical calibration procedure.

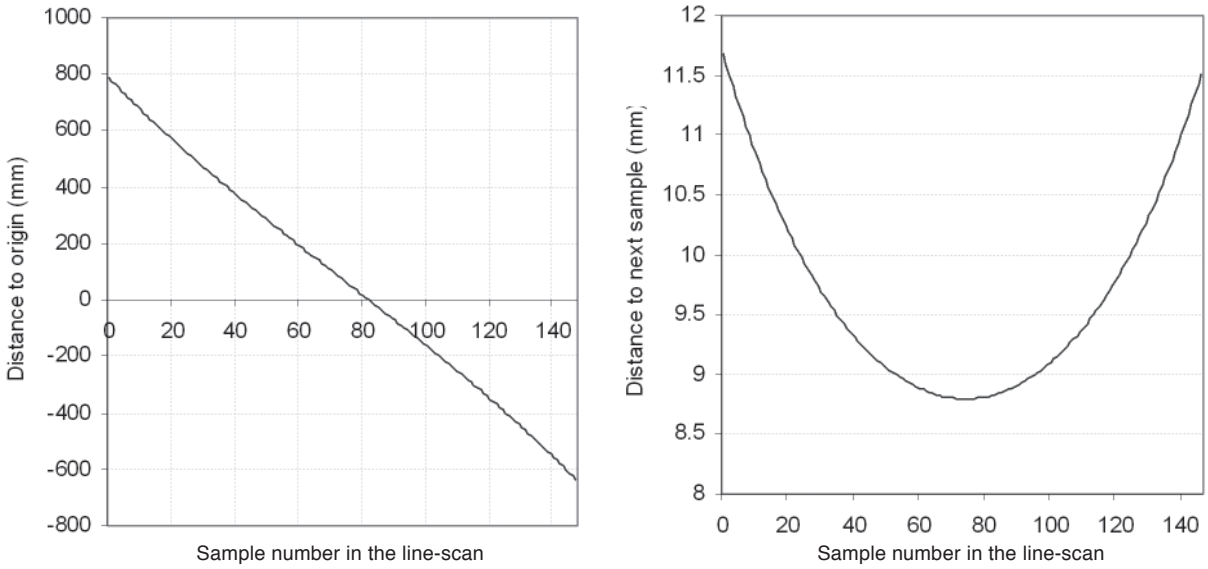

Figure 6. Relationship between sample number and distance to origin.

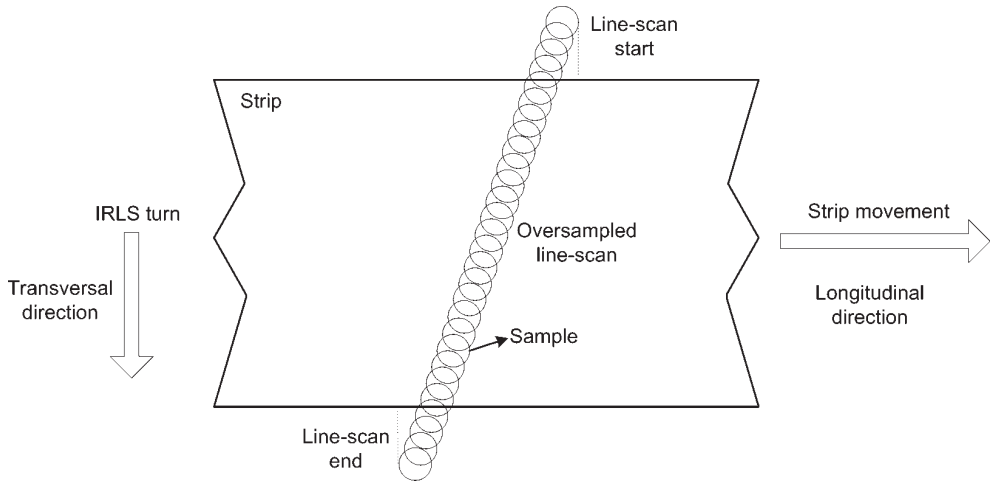

Figure 7. Line scan acquisition.

Filtering

The next step after acquisition is filtering. Filtering reduces the noise of the image in order to obtain a successful segmentation. Temperature measurement using non-contact sensors at high frequencies produces very noisy images.[1] For example, in the case of steel strip manufacturing, noise is caused mainly by the products sprayed on the strips to cool them. These products alter the surface emissivity of the steel, and provoke highly variable measurements.

To reduce the noise of the image, two filters are consecutively applied just after each line scan is acquired; one transversal and one longitudinal. Firstly, each line scan is filtered just after it is acquired with oversampling. This corresponds to the filtering of the 2D image in the transversal direction. Secondly, a new smoothed line scan is obtained by averaging (low pass filtering) the latest acquired line scan with the previous ones. This corresponds to filtering in the longitudinal direction of the 2D image. The reason for using two independent filters in both directions and not a bi-dimensional filter is because the samples of the two-dimensional image are not at the same distance in the transverse and longitudinal directions. The distance between adjacent samples in the same line scan (transverse direction) is approximately constant, but the distance between adjacent samples in successive line scans (longitudinal direction) varies with the speed of the continuous material and can be 30 times higher than the transversal distance.

When the acquisition rate of the A/D converter is high, the temperature at a specific position is measured by a set of adjacent samples, that is, oversampling occurs (Fig. 8). The higher the acquisition rate, the higher the oversampling carried out.

The filter in the transverse direction is based on overlapping samples acquired using the highest acquisition frequency possible in the system. Fig. 8 shows the transformation of an original line scan into the final line scan without overlapping. Once the line

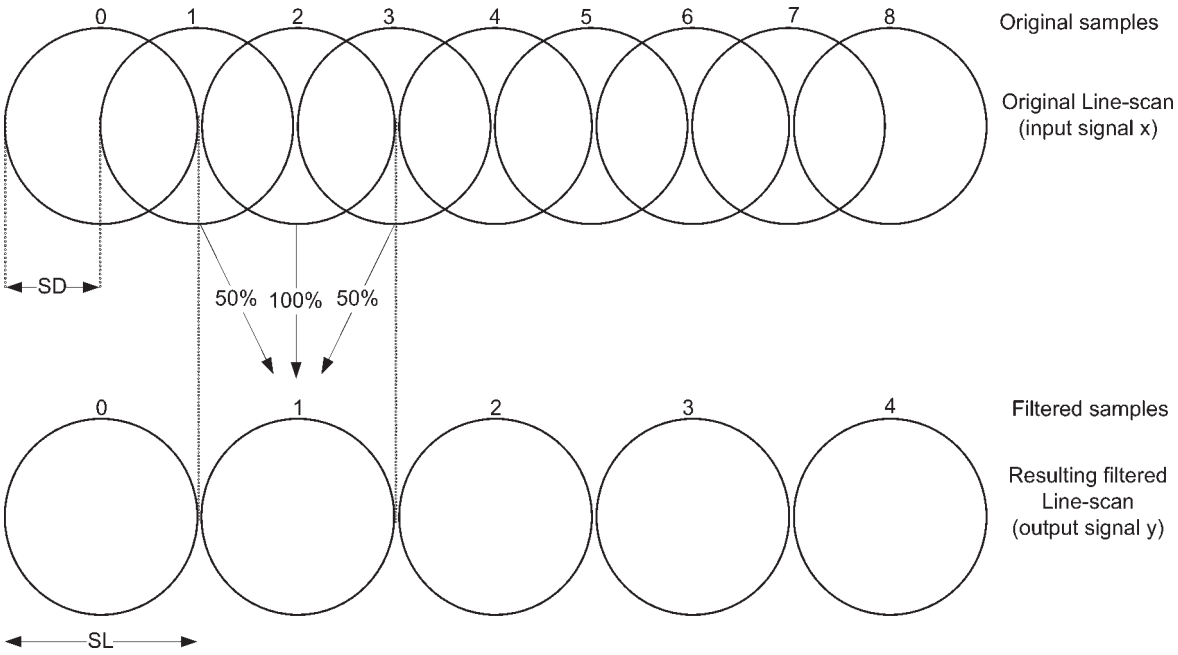

Figure 8. Transverse filtering process based on overlapping samples.

scan is acquired, the data is reduced to the minimum number of samples to fill the scan space without spatial overlapping.

In order to carry out the filtering process, a signal operator called SReF (Spatial Reduction Filtering) is defined. The operator input is an oversampled signal, $x[j]$, whose number of samples is N ($j = 0 \ldots N - 1$), and the operator output is a signal, $y[i]$, whose number of samples is M ($i = 0 \ldots M - 1$). The only restriction in the relation between N and M is that N must be greater than or equal to M.

Every sample in the output signal $y[i]$ is calculated using the samples from input signal x whose measurement space includes a part of the measurement space in the sample $y[i]$, that is, the samples of x which overlap $y[i]$, as can be seen in Fig. 8. This process involves two steps: first, determining the set of samples in signal x which overlap $y[i]$; second, for every sample in that set, calculating its weight in the calculation of the value of $y[i]$, which depends on the intersection degree of the samples in x with $y[i]$. For example, in Fig. 8, $y[1]$ should be calculated as is shown in Eq. (9).

$$y[1] = \frac{0.25x[1] + 0.5x[2] + 0.25x[3]}{0.25 + 0.5 + 0.25} \tag{9}$$

The set of samples in the signal x used to calculate $y[i]$ will be consecutive, that is, this set can be described by the first and last indexes of the samples of the signal x. Two variables will be used for this description: *SL* and *SD*. *SL* (sample length) is the diameter of the measurement space, which is a constant, defined both by the IRLS and by the working distance. *SD* (sample distance) is the distance from the beginning of a sample to the beginning of the next in signal x, and can be calculated using Eq. (10).

$$SD = \frac{M - 1}{N - 1} \tag{10}$$

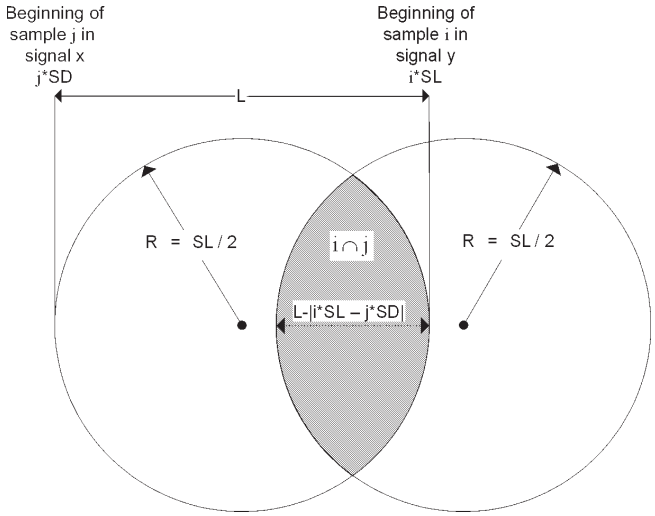

Figure 9. Intersection degree between two samples.

The first and last sample of the signal x which overlap $y[i]$ can be calculated using Eqs. (11) and (12), respectively, where *CIGT* means Closest Integer Greater Than, and *CILT* means Closest Integer Less Than. Both must take into account the different behavior in the borders.

$$First = CIGT\left(\frac{i * SL - SL}{SD}\right) \tag{11}$$

$$Last = CILT\left(\frac{i * SL + SL}{SR}\right) \tag{12}$$

To calculate the intersection degree between a sample in x and $y[i]$, the intersection area between these samples must be calculated. The problem lies in the

calculation of the shaded area of Fig. 9. Once the intersection area is obtained, it must be divided by the measured area of a sample (circle) to get the intersection degree in the range [0, 1].

Using the geometrical properties of the area measured in the samples (circles), the intersection degree (ID) can be calculated using Eq. (13), where the numerator represents the intersected area, and the denominator represents the area of the sample.

$$D(i,j) = \frac{SL^2 \arccos\left(\frac{SL^2 - SL|i*SL - j*SD|}{4}\right)}{16} - \frac{\left(SL - |i*SL - j*SD|\right)\sqrt{\left(\frac{SL}{2}\right)^2 - \left(\frac{SL - |i*SL - j*SD|}{2}\right)^2}}{8} \Bigg/ \pi\left(\frac{SL}{2}\right)^2 \quad (13)$$

Using both, the information from the samples in the signal x which overlap sample $y[i]$, and their intersection degree, the filtering operator can be calculated using Eq. (14). The denominator of the equation is used for normalization.

$$Iy[i] = SReF_{N,M,L}(x) = \frac{\sum_{j=CIGT(\frac{i*SL-SL}{SD})}^{j=CILT(\frac{i*SL+SL}{SD})} ID(i,j) * x[j]}{\sum_{j=CIGT(\frac{i*SL-SL}{SD})}^{j=CILT(\frac{i*SL+SL}{SD})} ID(i,j)} \quad (14)$$

In the longitudinal direction, the filtering is carried out by averaging line scans. To define the number of line scans to average, all the strips obtained during a typical manufacturing campaign were analyzed in order to find the highest gradient of temperature per longitudinal meter. The number of line scans averaged is selected as the maximum that allows the system to track the fastest temperature changes in the longitudinal direction without losing information. This number is calculated using the information provided by the messages received periodically from the process computer. Applying the two filtering we find that the steps space needed to store the data in memory and later in disk is reduced by 75%.

Segmentation

The segmentation of an image consists of the division of the image in a set of segments which have similar attributes, in this case, temperature. In this work, two segmentation algorithms are proposed and tested. Both are adapted versions of the well known approaches, region merging and edge based, which must work in real time on a stream of line scans.

The segmentation process for the type of thermographic images considered in this work differs in some aspects from the usual process carried out for images taken from the human visible spectrum. Usually, the segmentation process tries to extract objects from the image which correspond to real world objects. In this case, the result of the segmentation can be objectively assessed. Furthermore, in the case of thermographic images, the segmentation tries to find regions of homogeneous temperature, that is, regions formed by a set of adjacent line scans which have a similar temperature pattern. This makes the result of the segmentation much more difficult to assess, due to the inherent subjectivity of the homogeneity definition.

Different regions in the thermographic image appear as a consequence of the changes of the manufacturing conditions of the strip over time. The following is an example of how different regions can appear in an image. For an instant during strip manufacturing (Fig. 10, moment A) the speed is reduced, which produces a decrement in the temperature of the strip. Before the speed reduction the line scans acquired show a high line scan temperature pattern (Fig. 10, pattern 1), and after the speed reduction they show a lower one (Fig. 10, pattern 2). Later (Fig. 10, moment B) the speed strip is recovered and the pattern is again high (Fig. 10, pattern 3). After this, a typical change in the manufacturing conditions occurs (Fig. 10, moment C), which consists in the application of excessive pressure on one part of the strip. The excess of pressure generates heat and the temperature pattern rises where high pressure is applied to the strip (Fig. 10, pattern 4). When the excess of pressure disappears (Fig. 10, moment D) a flat temperature pattern appears again (Fig. 10, pattern 5). Finally, a new decrement of the speed (Fig. 10, moment E) produces a new temperature pattern (Fig. 10, pattern 6).

In summary, the segmentation procedure will group similar line scans in real time, producing, finally, a set of line scan temperature patterns.

The IRLS acquires line scans which contain thermographic information about the strip, (the foreground item of the image) and about the strip track (the background item of the image) as can be seen in Fig. 10. To extract the information about the strip from the image, a thresholding technique based on Ridler's algorithm is used before the segmentation algorithm is applied.

Region Merging Segmentation

Region merging segmentation methods search for adjacent regions within an image which meet some defined similarity criteria to merge them into a bigger one. One of the most important aspects in this kind of segmentation technique is how the similarity criterion is defined, which is mainly based on the description of the region. Several well-known similarity criteria for specific applications have been proposed.[6]

Region Description

The objective of the segmentation is to divide the image into a set of regions in real time. Since a region is a set of line scans with similar temperature attributes in the longitudinal direction, the region will be described by the average line scan of all the single line scans which belong to it. For every sample in the average line scan a confidence interval will be calculated using the average plus-or-minus the standard deviation of the average of each sample multiplied by a factor.

Algorithm

Initially, an empty region is defined, which will be considered the current region. Every time a new line scan is acquired the following steps are carried out:

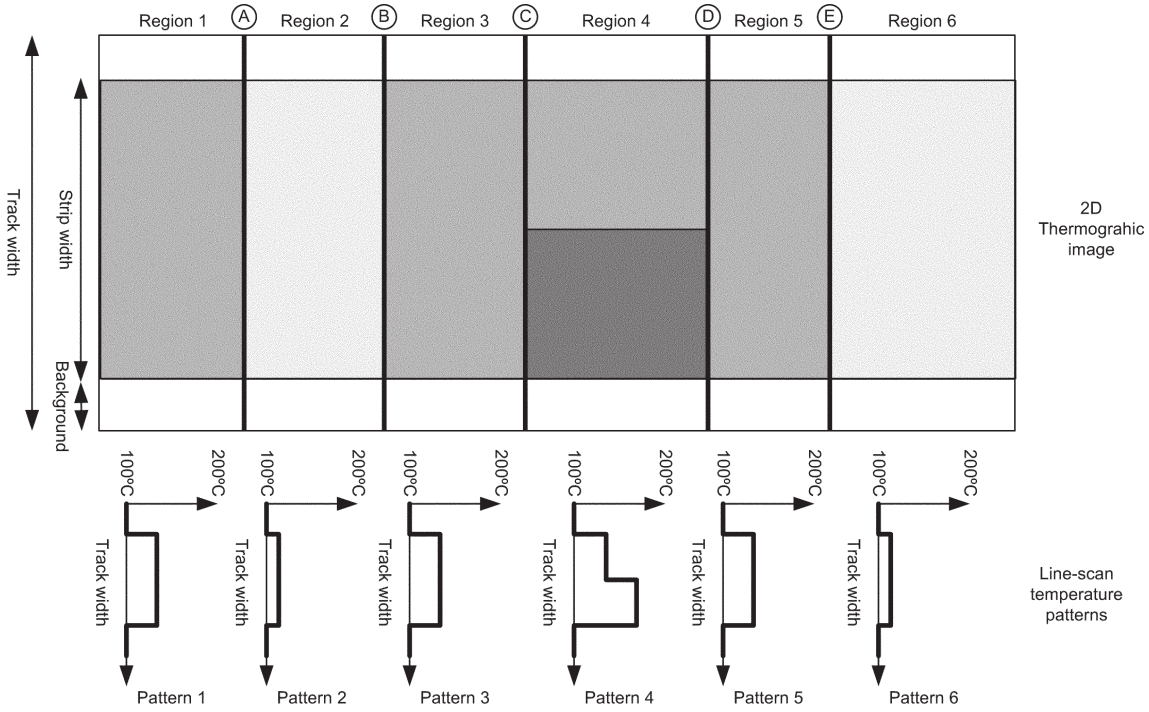

Figure 10. Thermographic image segmentation in regions with a similar line scan temperature pattern.

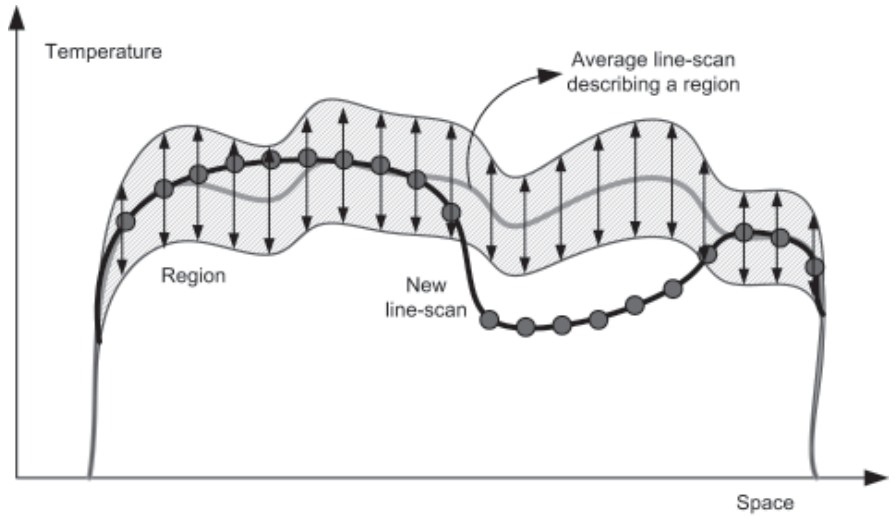

Figure 11. Homogeneity determination between a new line scan and a region.

- When the current region does not contain enough line scans for initialization purposes, the new line scan is merged with that region without homogeneity determination.
- Each sample in the new line scan has a corresponding sample in the region description. The number of samples in the new line scan which fall within the confidence interval of its corresponding sample in the region will be counted, and their percentage among all the samples in the new line scan is calculated.
- If the calculated percentage is greater than a determined threshold, the new line scan is said to be homogeneous with the region, and so, they are merged.
- To merge the new line scan and the region, the average line scan describing the region will be modified to include the new line scan in the average, that is, the region description will be re-calculated. This calculation can be done recursively, both for average and standard deviation, allowing a better performance for the real time implementation.

Figure 11 shows an example of the process of homogeneity determination between a new line scan and a region, where the new line scan, the average line scan describing the region, and the confidence interval for every sample in the region, are represented. In this example, 6 samples of 20 fall outside of their confidence interval, which means 20%.

Since there could be some very noisy line scans in the thermography acquired, a robust method has been

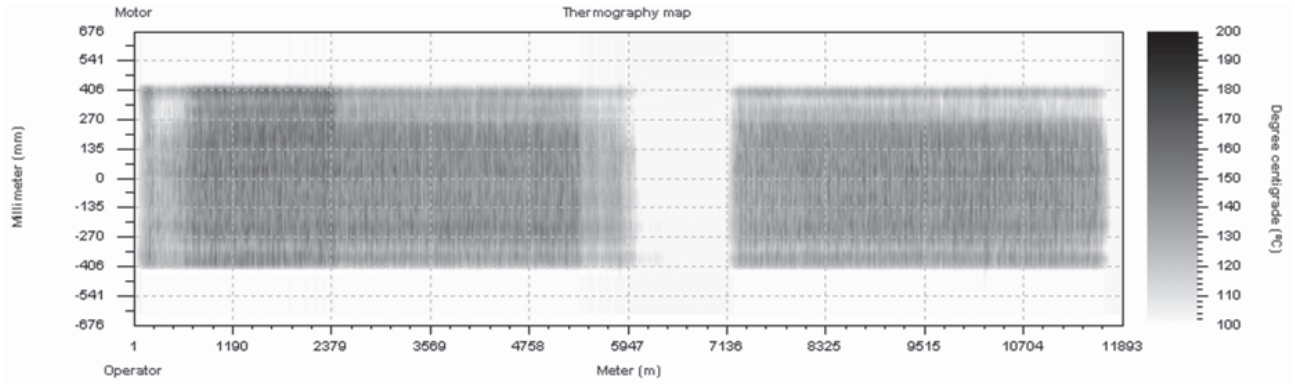

Figure 12. Typical thermographic image.

developed to decide when a new region appears. In this method, the terms "open region" and "closed region" will be used to identify when a region is able to include new line scans and when it is not, respectively.

When there is a new line scan not homogeneous with the current region, a new region is not automatically created. Instead, a transitory region is opened and the current region is not closed. Using successive line scans, the segmentation algorithm will check to see if the transitory region was created due to noise in the temperature signal or if it was the beginning of a real new region. This will depend on the homogeneity between the future line scans with the last open region, or with the transitory region. When there are a number of successive line scans homogeneous with the transitory region, the last open region is closed and the transitory region is converted to the new open region.

The configuration parameters of this segmentation algorithm are the following:

- The factor by which to multiply the standard deviation of the samples in the average line scan describing the region to obtain the confidence interval.
- The percentage threshold of samples which fall within the confidence interval of its corresponding sample in the region among all the samples in the line scan.
- The number of line scans in a region that will be merged without any homogeneity determination for initialization purposes.
- The necessary number of homogeneous line scans in a transitory region to be considered as a real region.

Edge Based Segmentation

Edge based segmentation techniques rely on edges found in an image by edge detection operators. These edges mark image discontinuities regarding some image attribute. Usually, the attribute used is the luminance level; in this case, the temperature level will be used.

The general edge based segmentation process consists of several steps. It starts by applying a convolution kernel (or gradient operator) over an image.[7] The result obtained from the convolution is the gradient of the image, which is obviously dependent on the gradient operator used. The next step involves the analysis of the gradient in order to eliminate the noise while keeping the real edges. Usually, this process is carried out by using thresholding techniques or morphological operators. The last step consists of linking the edges in order to determine the boundary of the regions,[7] and in this way, to accomplish the segmentation of the image in regions.

In the new algorithm presented in this article, the segmentation is carried out in real time. However, a delay is necessary in the edge detection, since to calculate the gradient in a longitudinal position, the gradient operator needs line scans previous and posterior to that position. The number of line scans needed depends on the size of the operator. Fig. 12 shows a typical final two-dimensional thermographic image which will be used to show the steps involved in the edge based segmentation.

Edge Operator

One of the most important issues in the edge based segmentation is the selection of the gradient operator. Many different gradient operators have been analyzed in the literature.[7] The selection of the operator depends mainly on two aspects: the expected direction of the edge and the edge profile. With regard to the first aspect, and keeping in mind that the objective of the segmentation is to divide the image longitudinally, it can be stated that the edge detector applied will only search for edges in the longitudinal direction, that is, from left to right in Fig. 12.

The edge profile in the analyzed thermographic images could be classified as a noisy ramp. Fig. 13 shows an edge profile obtained from the center of the image shown in Fig. 12 where ramps and edges can be appreciated. After examining different edge types, it was concluded that neither the slope nor the height of the ramps were constant, so this information cannot be used in the design of the edge operator.

Different gradient operators were tested to choose the best suited for this kind of edge profiles, including Boxcar (extended Prewit), LoG (Laplacian of Gaussian) and FDoG (First Derivative of Gaussian).[7] In Fig. 14 and Fig. 15 the gradients obtained after applying the Boxcar and FDoG operators can be seen.

Projection of the Gradient

Once the edge operator is applied, a gradient for the image is obtained. The next step of the segmentation is the projection of the gradient onto the londitudinal axis. This step simplifies the thresholding that must be carried out to eliminate the noise from the gradient.

Figure 16 and Fig. 17 show the projection of the gradients obtained using the Boxcar and FDoG gradient operators. As can be seen, the Boxcar operator seems to identify the edges of the image more clearly and with more response per edge, which corroborates the conclusions drawn by Canny[8] about the proper gradient operator under his constraints of SNR (signal to noise ratio) and simple response.

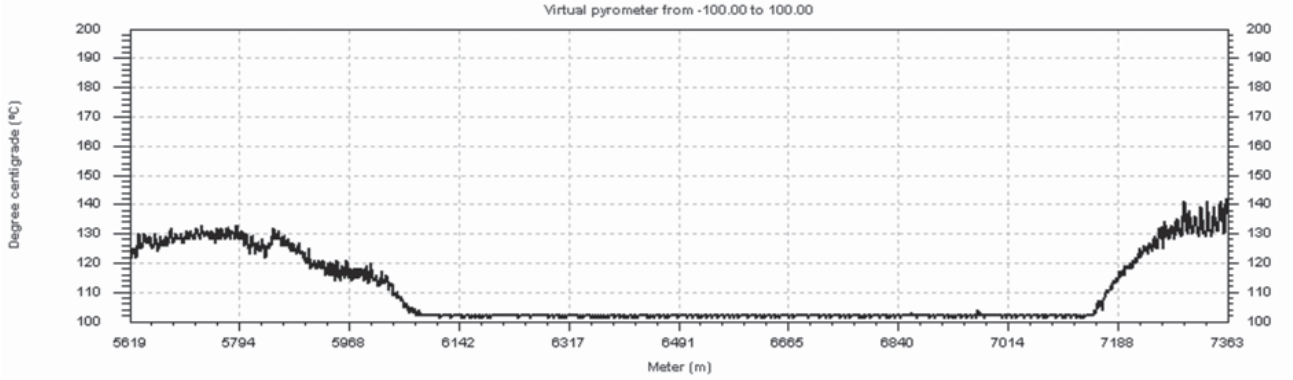

Figure 13. Edge profile.

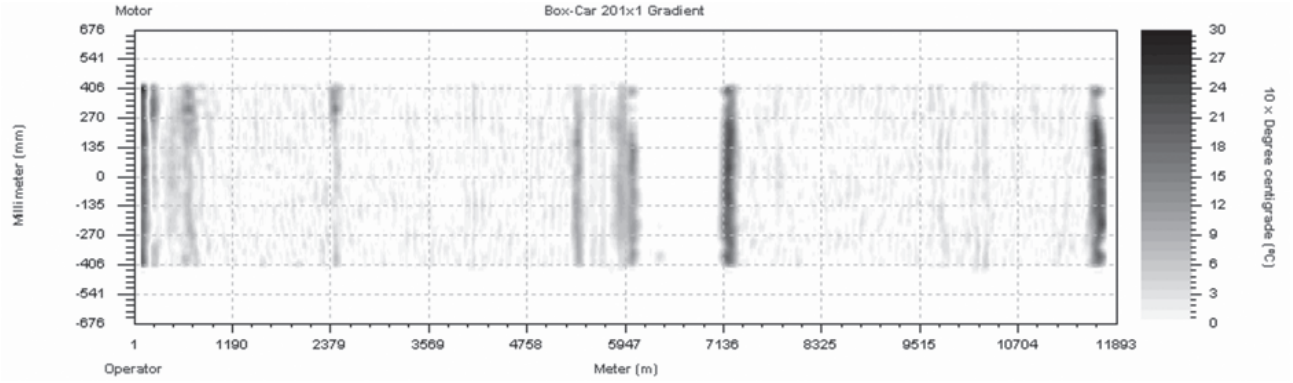

Figure 14. Gradients obtained from Boxcar edge operator.

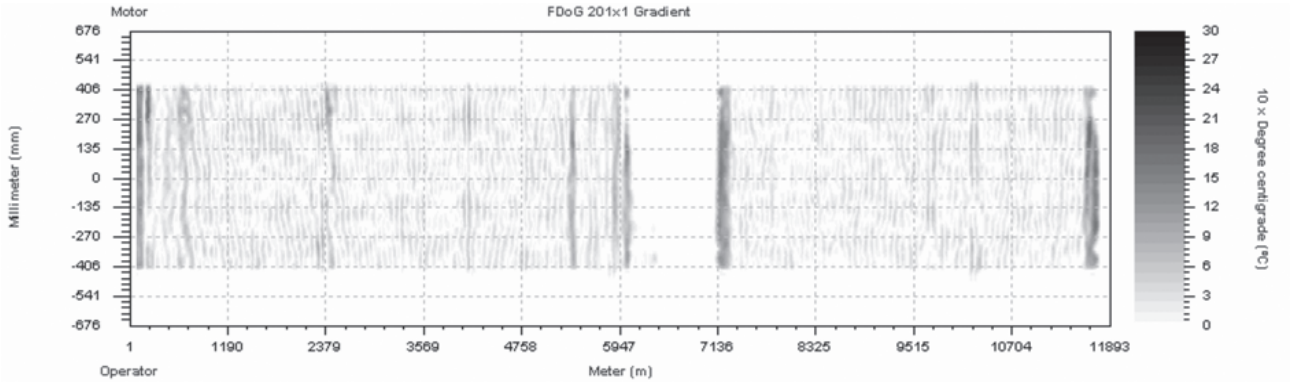

Figure 15. Gradients obtained from FDoG edge operator.

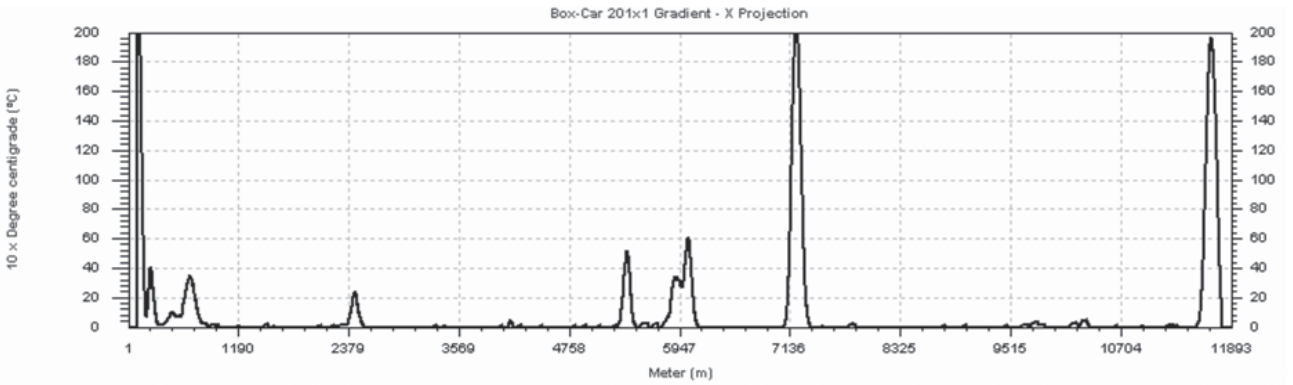

Figure 16. Projection of the gradient obtained from Boxcar edge operator.

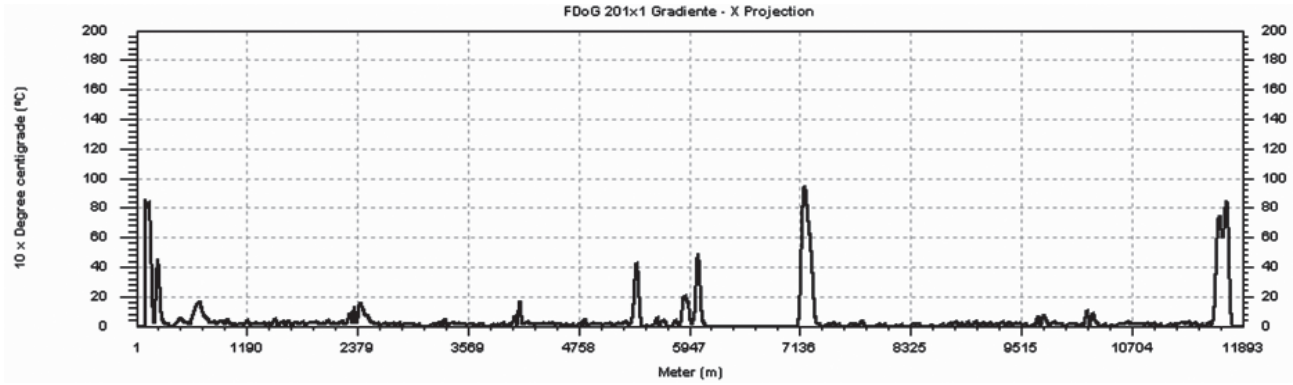

Figure 17. Projection of the gradient obtained from FDoG edge operator.

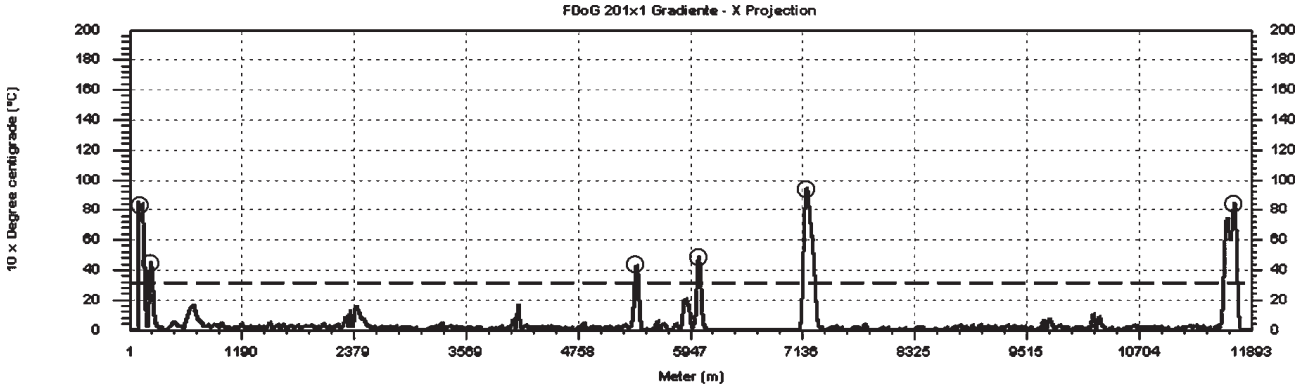

Figure 18. Thresholding of the projection of the gradient.

Thresholding

Once the projection of the gradient is available, it is thresholded. The objective of the thresholding is to differentiate noise from real edges. An edge is inferred when there is data in the projection over the threshold value. When adjacent edges are found (adjacent values of the projection over the threshold), only the edge with the higher value in the projection of all of the adjacent positions will be considered, which can be interpreted as a morphological operator.

Figure 18 shows an example of the thresholding carried out over a projection of a gradient. As can be seen, the noise is under the threshold value and edges are obtained from the peaks over it. Only the highest value of each peak will be considered to establish the longitudinal position of its corresponding edge.

Summary

Although the projections obtained (Fig. 16 and Fig. 17) from the generated gradients (Fig. 14 and Fig. 15) from the two operators are different, the positions obtained for the edges after the thresholding were quite similar. In fact, the main difference between both edge operators is their behavior in the presence of noise, and this effect is eliminated when positions are only considered as the tops of the peaks in the thresholding. Since different operators produced a similar result, Boxcar is used because its recursive implementation was faster than the others. Finally, the operator used is the following:

$$[-1 \;\; -1 \;\; \cdots \;\; -1 \;\; -1 \;\; 0 \;\; +1 \;\; +1 \;\; \cdots \;\; +1 \;\; +1]$$

A two-dimensional operator is not used because it would require a longer execution time without a noticeable improvement on the final result.

The configuration parameters of the algorithm are the following:

- The length of the edge operator.
- The threshold used to extract the edges in the projection.

Segmentation Assessment

Since segmentation is one of the most important steps of image processing, its accuracy must be assessed. Segmentation assessment determines the effectiveness of an algorithm, allows the comparison of several algorithms, and the tuning of the configuration parameters of a specific algorithm. In recent decades, many segmentation algorithms have been developed for different kinds of applications. However, less effort has been made in their evaluation.

Zhang[9] proposes a classification of existing assessment methods as "analytical", "empirical goodness", and "empirical discrepancy". Yang[10] proposes a different classification as "supervised" and "unsupervised". The "unsupervised" group of Yang's classification corresponds to the "analytical" group of Zhang's classification; "supervised" corresponds to the others.

- "Analytical" methods attempt to characterize an algorithm by itself in terms of principles, requirements, complexity, etc. without any reference to a concrete implementation of the algorithm or test data, such as the time complexity or the response to a theoretical data model.

- "Empirical goodness" methods evaluate algorithms by computing a "goodness" metric on the segmented image without *a priori* knowledge of the desired segmentation result. For example Levine,[11] uses intra-region gray level uniformity as his goodness metric.
- "Empirical discrepancy" methods calculate a discrepancy measurement between the result of the segmentation algorithm, and the desired correct segmentation for the corresponding image. In the case of synthetic images, correct segmentation can be obtained automatically from the image generation procedure, while in the case of real images it must be produced manually by an experienced operator. Many discrepancy metrics have been proposed, some of them treat segmentation as a classification problem where each pixel is associated to a correct class (usually edge and non-edge).[12,13] Other methods calculate the distance between mis-segmented pixels and the nearest correctly segmented pixels.[7,12]

In order to apply the proper assessment method to the segmentation of the thermographic images being analyzed, the following requirements are established:

1. The set of ideal edges between regions for each image must be known, so that errors in the segmentation can be detected and assessed one by one.
2. The assessment procedure must produce a continuous magnitude, so the adjustment of the parameters of the segmentation algorithm can be carried out accurately.
3. Due to the length of the thermographic images and to the existing noise, there will be a degree of uncertainty in the determination of the edge position by the experienced operator; therefore, the assessment method needs to take the uncertainty of the ideal segmentation into account.
4. The values of the magnitude generated by the assessment procedure must be limited to a range, so they can be analyzed and compared easily.
5. The assessment method must weigh up the error committed to detect each edge using the distance between the detected edge and the real edge. However, this must only happen when the position of the detected edge is in the influence area of the position of a real edge (when both positions are close enough), and also when that real edge is closer to the detected edge than any other.

Since none of the available segmentation assessment methods fit all these requirements, a new one will be proposed, which can be classified as an "empirical discrepancy" method.

When the performance of a segmentation algorithm is determined empirically, it is necessary to use an ideal segmentation, usually known as the ground truth. The ideal segmentation defines the optimum result of the segmentation.

Some authors, like Yitzhaky,[14] propose the creation of the ground truth based on a set of automatic segmentations. However, it seems difficult to determine the right parameters to choose in these automatic segmentations. Yitzhaky uses a statistical approach to provide a discrepancy metric.

In our work, a set of 30 real images are used as a test set to assess the segmentation results. Although the creation of the ideal segmentation of each real image must be manual, and thus, time consuming, it avoids the problems derived from the validation of synthetic images. It is important to note that synthetic images should represent real images; therefore, some kind of validation should be carried out. In order to obtain the ideal segmentation for each image, several experienced operators were employed to compensate for the subjectivity of finding the edges in the images. Each of the operators provided an ideal segmentation for each image in the test set.

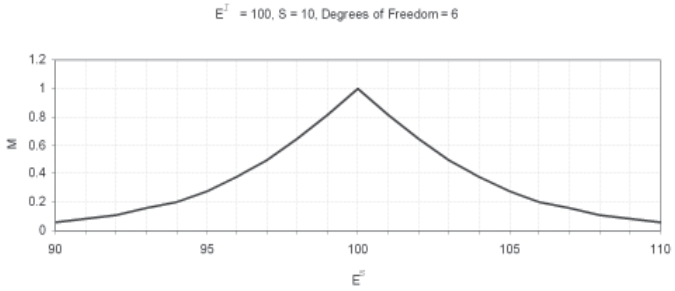

Figure 19. Match function for the edge comparison.

After the experts provided the ideal segmentation for each image, the next step consists of defining a single ideal segmentation for each image, where only those edges established by more than half of the experts will be considered. The data for each edge in the ideal segmentation will include: the average of the positions established by the experts, the standard deviation of the average position, and the number of experts who established that edge. Once the ideal segmentation is available, a discrepancy metric is calculated between the ideal segmentation and the segmentation produced by the algorithm using a match function applied to each edge. The match function proposed in this work is based on the statistical properties of the ideal segmentation established by the experts.

Considering the set of positions established by the experts for each edge as a set of independent observations, we can expect that the average position of the edges follows a normal distribution if the number of experts is more than 30. If the number of experts is under 30 (the case presented here), the average of the position of the edges follows a Student's t-Distribution with $n - 1$ (number of experts less 1) degrees of freedom. To compare the distribution of the position of one edge provided by the experts with the position of the edge provided by the segmentation algorithm, the P-Value, which measures the significance level, provides an optimal statistical method. So, the match function (M) of an edge using statististical properties is that shown in Eq. (15), where E^I is the average of the ideal edge position, S is the standard deviation of that average, E^S is the position of the found edge by the algorithm, and n is the number of experts.

$$M(E^I, E^S) = P\left\{\frac{\left|E^I - E^S\right|}{\frac{S}{\sqrt{n}}}\right\}_{n-1} \tag{15}$$

Figure 19 shows an example of a graphical representation of the match function for E^I equal to 100, S to 10, and 6 degrees of freedom.

Once the match function is specified for each edge of the image, the segmentation empirical assessment metric (SEAM) of a whole image can be expressed as (16), where NE is the number of edges in the ideal

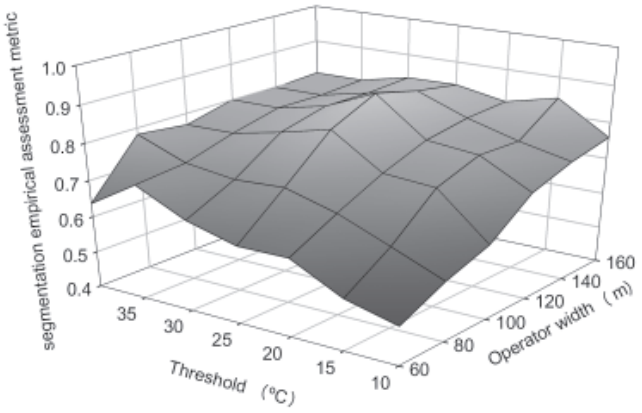

Figure 20. Results of the edge based algorithm.

segmentation, and NF is the number of edges found. Equation Eq. (16) can be seen as a joint probability of error since it takes into account the two kinds of errors which can occur in the segmentation: non-existing edge detected (false detection) and existing edge non-detection (missed detection).

$$SEAM = \frac{\left(\sum_{i=0}^{NF} M(E_i^I, E_i^S)\right)^2}{(NE \cdot NF)^2} \tag{16}$$

This assessment method fits all the requirements previously established since it takes uncertainty into account, is continuous, and is limited to the range of [0,1] (where a value of unity means perfect segmentation).

Results

The performance of both segmentation algorithms must be assessed using the new assessment method, for which a set of images was selected. The selected test image set included images with different patterns of temperature changes. The test set was manually segmented by a group of seven experts using a software tool to carry out the segmentation more easily.

All the images in the selected test set were segmented by the two proposed algorithms with different values for their configuration parameters. The procedure is based on a complete factorial experimental design. The number of different combinations of parameters for the region merging algorithm was 1728 for each image. The number of different combinations of parameters for the edge based algorithm is 144 for each image. This lower number is due to the lower number of parameters of the second algorithm.

The segmentation of the test image set using the region merging algorithm provided a value for the segmentation empirical assessment metric (SEAM) of between 0 and 0.78, where only five combinations of the configuration parameters produced a SEAM of over 0.7. The optimal configuration parameters were 2.25 as the multiplying factor, 70 as the percentage threshold, 60 initialization line scans, and 60 line scans to consider a transitory region as a real region. The importance of the method for opening and closing regions was demonstrated when tests were carried out without including it and the maximum of the SEAM decreased to 0.13.

The segmentation of the test image set using the edge based algorithm provided a value for the SEAM of between 0 and 0.88 where most of the combinations of the configuration parameters produced a SEAM of over 0.75. The optimal configuration parameters were 120 as the operator length, and 25 as the threshold of the projection gradient. Fig. 20 shows the SEAM values produced by the edge based segmentation algorithm.

The edge based segmentation algorithm performs better than the region merging algorithm, of the best 25 configurations of both algorithms, 23 correspond to the edge based algorithm. Also, it is more robust since it reached a correct segmentation for nearly all of the strips. Robustness is an important issue for industrial applications. To assess robustness, a large number of images taken from strips manufactured in different months were segmented using the edge based algorithm. After this, a small random percentage of images were reviewed, showing an appropriate segmentation for all of them

The length of the operator used in the edge based algorithm introduces a delay of 6 seconds in the detection of the edge, which in a strip whose processing lasts about 8 minutes, is an acceptable delay.

During the segmentation process, the thermographic image is divided into a set a regions, each of them representing a line scan pattern, which is available in real time as soon as the edges of the regions are detected. Figure 21 shows the segmentation of the image shown in Fig. 12 along with the different line scan patterns obtained. In this figure each line scan pattern is shown with a polynomial fit, which could be used as a compact description of the pattern.

After all the layers of the system have been developed, the next step is to analyze the real time performance of the whole system. There are two sets of tasks in the system, the first set will be called acquisition pipeline; it is triggered at every sensor turn, and will be executed at high priority. The second set will be called segmentation pipeline; it is triggered when a message from the process computer is received with the current strip length and speed, and will be executed at a lower priority.

Tasks in the acquisition pipeline are sequentially executed after the activation of the digital line which indicates the beginning of the scan valid angle in the thermographic sensor. These tasks are the following:

- Acquisition: this task is carried out in the A/D board, using a thermographic sensor of 80 Hz: A new line scan is ready to be acquired every 12.5 ms (at every turn of the sensor), which means acquisition will take 2.086 ms, that is 1/6 of the whole turn, the scan valid angle. After the acquisition is finished, the board sends an interrupt to notify it to the system.
- Interrupt latency: the interrupt sent when the acquisition finishes is received by the operating system, which forwards it to the board driver. The driver notifies the user developed acquisition software through a callback procedure. This task is carried out mainly in the OS.
- Acquisition rearming: when the callback procedure in the user developed acquisition software is executed, two minimum actions are carried out: the line scan acquired is stored in a circular buffer; and the acquisition is rearmed.
- Transversal filtering: this task is blocked until there is a new line scan available in the acquisition circular buffer (input). This task applies the filter defined by Eq. (14) and stores the result in a new circular buffer.

The interaction of all these tasks can be seen in the sequence diagram in Fig. 22, where the vertical

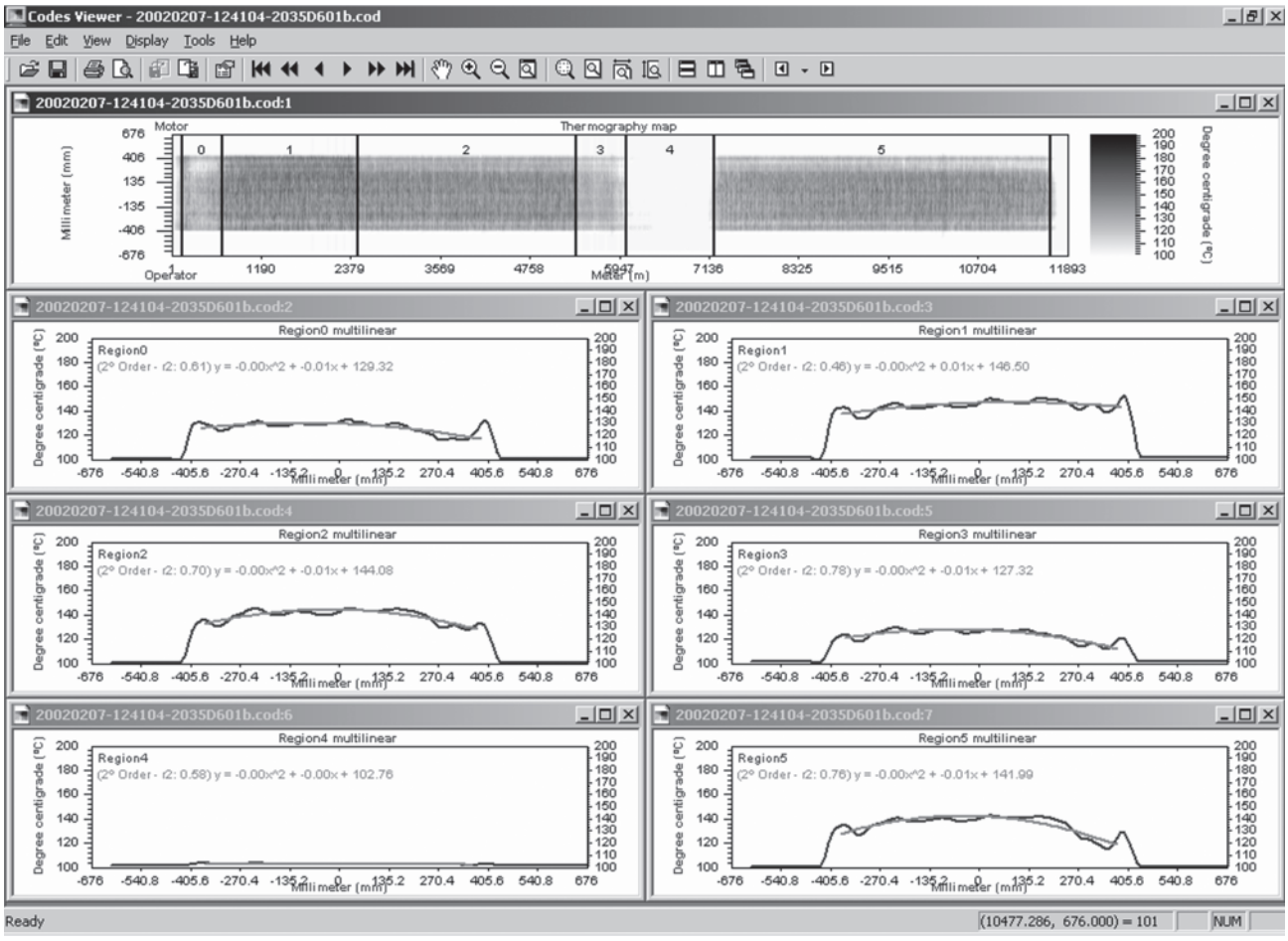

Figure 21. Description of the segmentation.

dimension representing time is only approximate for the sake of simplicity on the figure.

Tasks in the segmentation pipeline are sequentially executed only when a message from the process computer is received (every 500 ms approximately), including the current strip length and speed, since only then is there information to carry out the longitudinal filtering and thus the segmentation. This set of tasks is run at a lower priority than the tasks in the first set. The tasks are the following:

- Longitudinal filtering: this task filters longitudinally the line scans using the information about the speed and length of the strip and produces a set of longitudinally filtered line scans. Both line scans input and output are stored in circular buffers.
- Segmentation: blocked until there is a new longitudinally filtered line scan available in the longitudinal filtering circular buffer (input). This task applies to each line scan the segmentation process described above.

The interaction of all these tasks can be seen in the sequence diagram in Fig. 23, where the vertical dimension representing time is only approximated for the sake of simplicity on the figure.

Table I shows the average execution time of the tasks running on a Pentium 3 computer at 1 GHz with 512 MB of RAM.

Figure 24 shows the chronogram of the system operation, where the execution time of the tasks is only represented in an approximate manner in order to simply the figure. Labels A, B, and C, are used to indicate that there are different cases of CPU competition in the execution of both pipelines. In case A there is no CPU competition. Case B shows a possible parallelism where tasks in the segmentation pipeline are executed during the acquisition, but where there is no CPU competition either since the acquisition task is carried out by the A/D board (task represented by the filled bar). Case C shows how tasks in the segmentation pipeline are preempted by the higher priority tasks in the acquisition pipeline if their execution overlaps.

TABLE I. Tasks of the System

	Task	Measured time	
Acquisition pipeline	Acquisition	2.083 ms	4.64 ms
	Interrupt latency	2.5 ms	
	Acquisition rearming	0.0002 ms	
	Transversal filtering	0.060 ms	
Segmentation pipeline	Longitudinal filtering	0.178 ms	0.23 ms
	Segmentation	0.050 ms	

The interrupt latency is very high because of the lack of determinism of the operating system used, Win2000. It is important to note that if the interrupt latency lasts more than 10.4 ms, the A/D board will not be rearmed before the deadline and a line scan will be missed.

After many tests under extreme circumstances it can be concluded that the system is able to manage all the

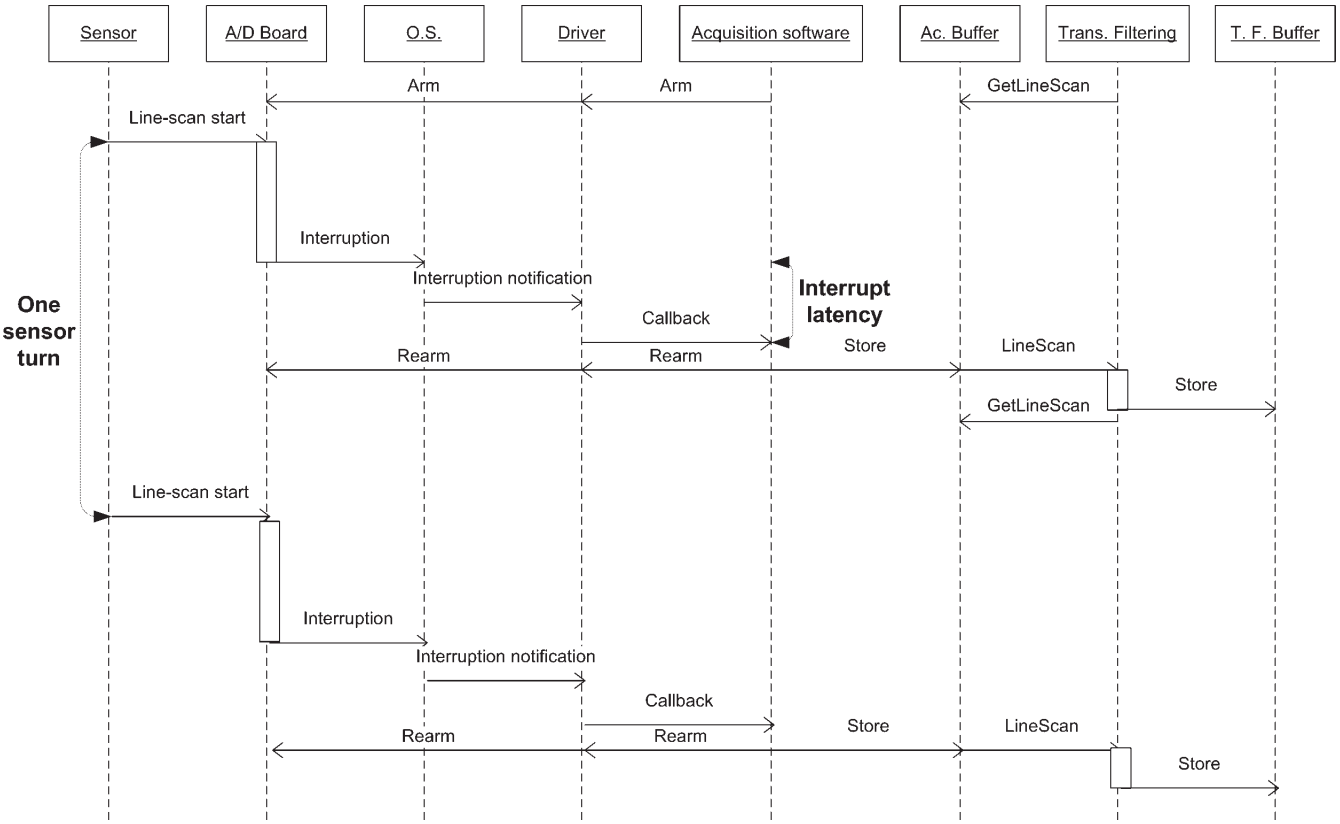

Figure 22. Sequence diagram of the acquisition pipeline.

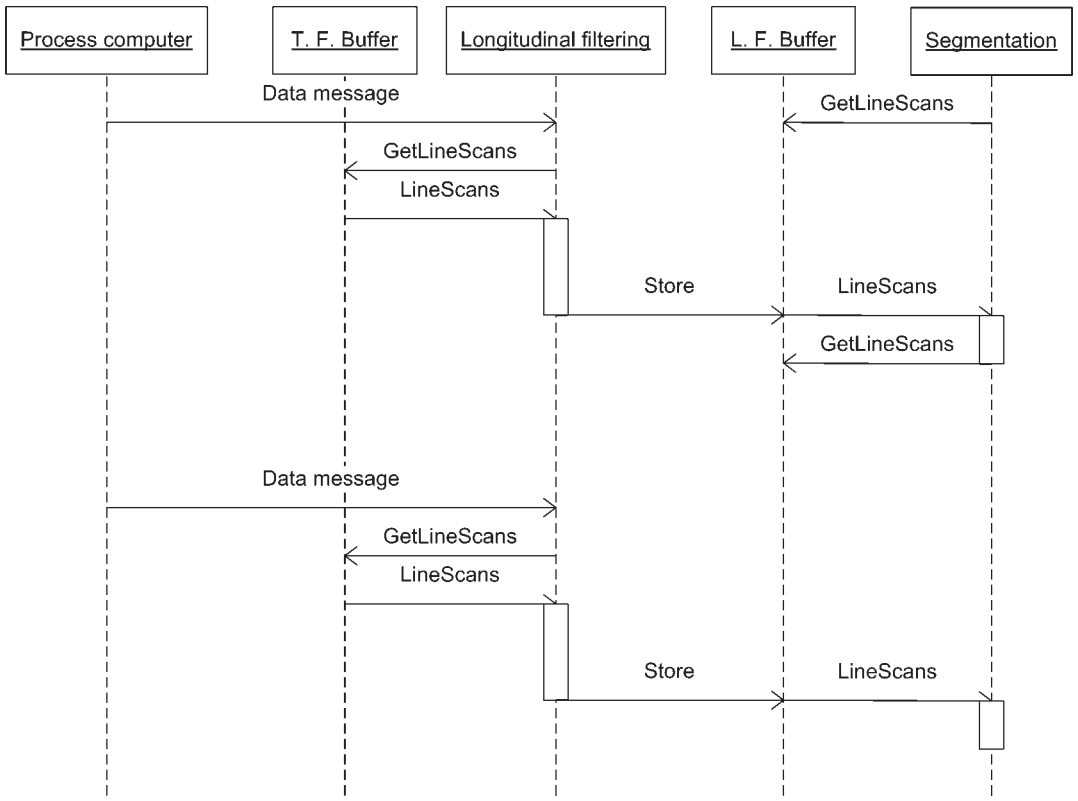

Figure 23. Sequence diagram of segmentation pipeline.

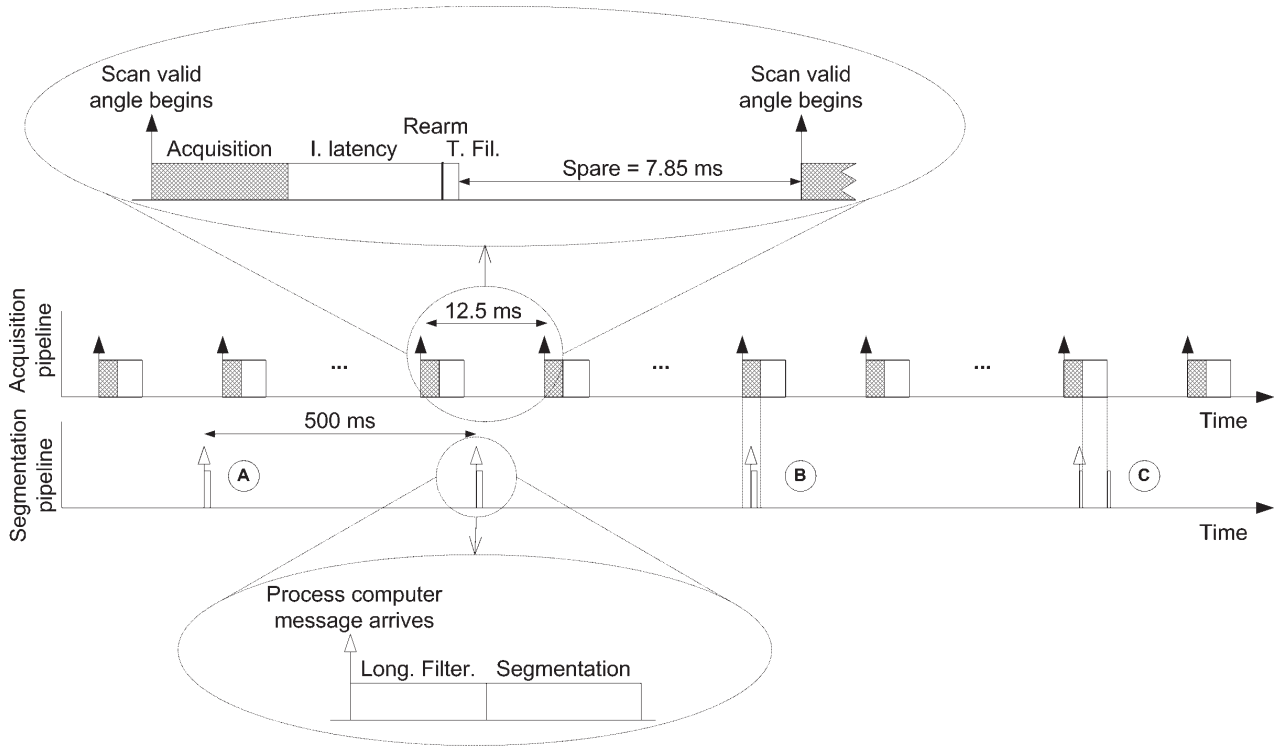

Figure 24. Chronogram of the system operation.

tasks without missing line scans, being able even to use a thermographic sensor with a higher frequency. The use of circular buffers to communicate tasks proved its efficiency as a proper mechanism to handle spurious delays in the task execution time probably caused because of the lack of determinism in the operating system used.

Conclusions

In this article, new algorithms for real time acquisition, filtering and segmentation of thermographic images have been proposed and assessed. Calibration procedures for temperature and spatial scale have also been developed. Two different segmentation algorithms have been proposed, and to measure their performances, a novel segmentation assessment method based on the uncertainty of the ideal segmentation was developed and applied. The assessment method allowed a clear identification of the best segmentation algorithm of the two proposed initially, that is, edge based segmentation.

Segmentation produces a set of line scan patterns which describe the thermographic behavior of a manufactured strip and detects changes in the line scan pattern in real time. As soon as a new line scan pattern is detected, and only then, the pattern change is sent to the control loop of the manufacturing process. Only sending patterns change leads to smoother and more effective process control than sending the entire line scan sequence. Segmentation is also very important, in order to carry out data mining over large image sets.

Another line of investigation is the description of each region in a reduced way. Current research shows that one of the best methods could be the polynomial fit.

References

1. P. Foulkes, *Toward Infrared Image Understanding*, PhD Thesis, Oxford University, Oxford, UK, 1991.
2. A. D. H. Thomas, M. G. Rodd, J. D. Holt, and C. J. Neill, Real time industrial visual inspection: A review, *Real Time Imaging* **1,** 139 (1995).
3. B. G. Batchelor and P. F. Whelan, *Selected Papers on Industrial Vision Systems*, SPIE Milestones Series, SPIE, Bellingham, WA, 1994.
4. T. S. Newman and A. K. Jain, A survey of automated visual inspec tion, *Computer Vision and Image Understanding* **61,** 262 (1995).
5. P. K. Sahoo, S. Soltani and A. C. K. Wong, A survey of thresholding techniques, *Computer Vision, Graphics and Image Processing* **41,** 233 (1998).
6. R. M. Haralick and L. G. Shapiro, Image segmentation techniques, *Computer, Vision, Graphics, and Image Processing* **29,** 100 (1985).
7. W. K. Pratt, *Digital Image Processing*, 2nd ed., John Wiley and Sons, New York, 1991.
8. A. Canny, A computational approach to edge detection, *IEEE Trans. Pattern Anal. Machine Intell.* **8,** 769–698 (1986).
9. Y. J. Zhang, A survey on evaluation methods for image segmentation, *Pattern Recognition,* Elsevier Science **29,** 1335 (1996).
10. L. Yang, F. Albregtsen, T. Lonnestad, and P. Grottum, A supervised approach to the evaluation of image segmentation methods, *Proc. CAIP*, 759-765 (1995).
11. M. D. Levine and A. Nazif. Dinamic measurement of computer generated image segmentations, *IEEE Trans. Pattern Anal. Machine Intell.* **7,** 155 (1985).
12. W. A. Yasnoff, J. K. Mui, J. W. Bacus, Error measures for scene segmentation, *Pattern Recognition* (Elsevier Science) **9,** 217 (1977).
13. S. U. Lee, S. Y. Chung and R. H. Park, A comparative performance study of several global thresholding techniques for segmentation, *Computer Vision, Graphics and Image Processing* **52,** 171 (1990).
14. Y. Yitzhaky, E. Peli, A method for objective edge detection evaluation and detector parameter selection, *IEEE Trans. Pattern Anal. Machine Intell.* **25,** 1 (2003).